Table of Contents Appendix Figures and Tables:

Appendix Figures:

Appendix Figure S1.....2

Appendix Figure S2.....3

Appendix Figure S3.....4

Appendix Figure S4.....5

Appendix Figure S5.....6

Appendix Tables:

Appendix Table S1.....7

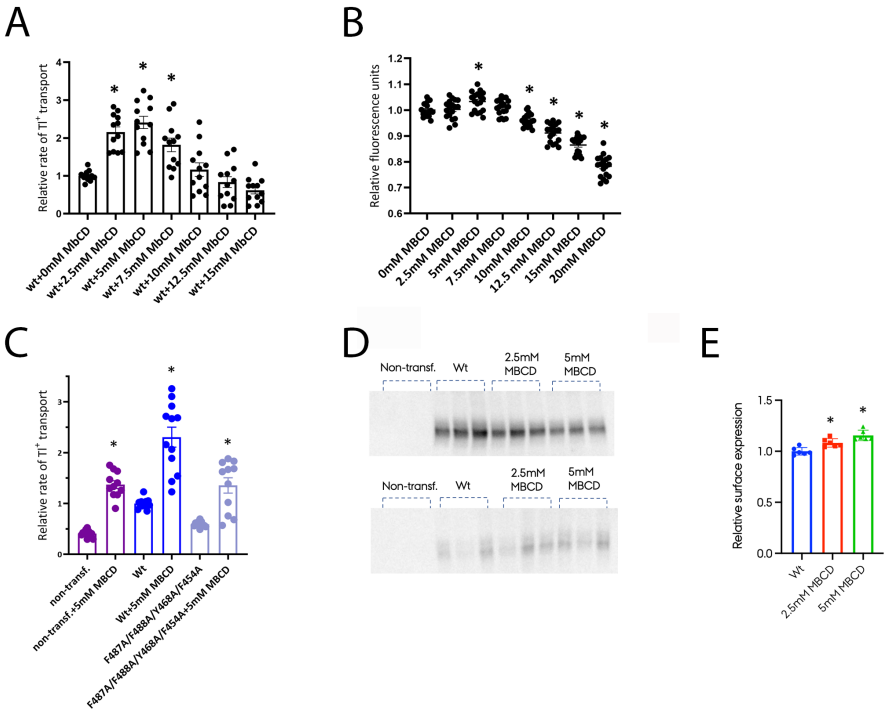

Appendix Figure S1: Effects of cholesterol depletion on transport properties of wt NKCC1 and F487A/F488A/Y468A/F454A mutant. A) Relative rate of Tl^+ transport in GripTite HEK293 MSR cells expressing wt NKCC1 treated with various concentrations of MβCD for 30 min at 37˚C followed by 1 h at RT. Data are means ± S.E.M. (n=12). Significance is assessed by One-way ANOVA followed by Dunnet's multiple comparisons test (*P<0.05). B) Viability of GripTite HEK293 MSR cells after treatment with MβCD for 30 min at 37˚C followed by 1 h at RT. Viability is measured as the ability of the cells to reduce the non-fluorescent resazurin to the highly fluorescent resorufin. Data are means ± S.E.M. (n=18). Significance is assessed by One-way ANOVA followed by Dunnet's multiple comparisons test. C) Relative rate of Tl^+ transport in non-transfected (non-transf.) GripTite HEK293 MSR cells, or cells expressing wt, or F487A/F488A/Y468A/F454A NKCC1 treated with 5mM MβCD for 30 min at 37˚C followed by 1 h at RT. Data are means ± S.E.M. (n=12). Significance between each group is assessed by One-way ANOVA followed by Dunnet's multiple comparisons test (*P<0.05). D) Representative immunoblots of wt NKCC1 in membrane fractions (upper blot) and total lysates (lower blot) from GripTite HEK293 MSR cells transfected with wt NKCC1 and treated with 2.5 mM or 5 mM MβCD for 30 min at 37˚C followed by 1 h at RT. E) Semi-quantitative assessment of the membrane abundance of wt NKCC1 expressed in GripTite HEK293 MSR cells treated with 2.5mM and 5mM MβCD for 30 min at 37˚C followed by 1 h at RT normalized to total NKCC1. The membrane abundance is quantified by densitometry of Western blot with 6 replicas. Data are means ± S.E.M.

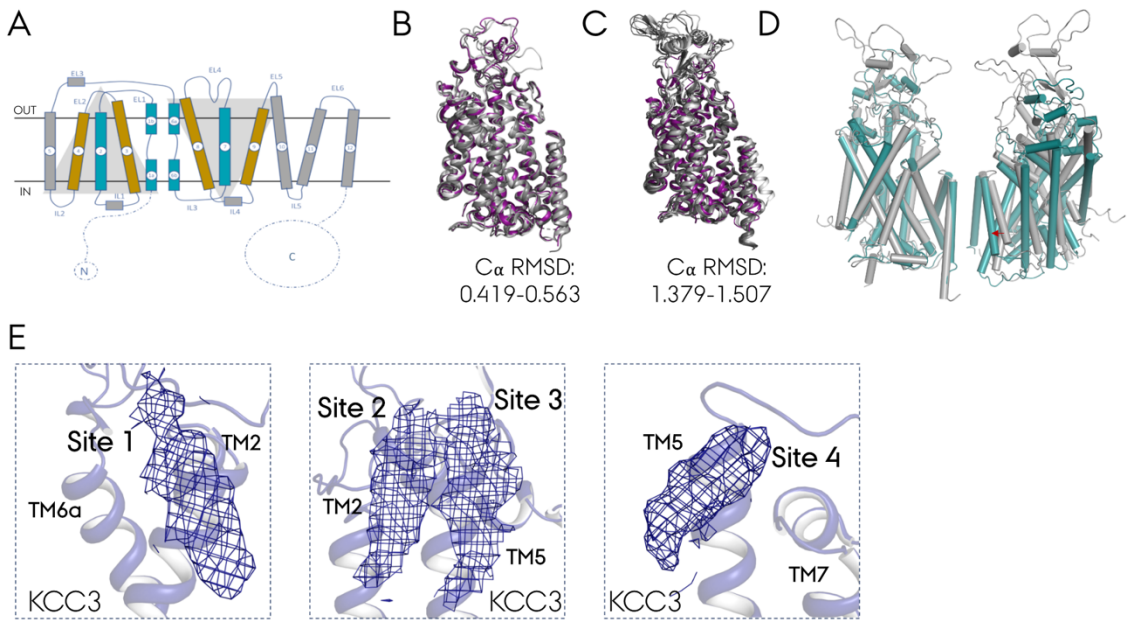

Appendix Figure S2: Comparison of the hNKCC1 structure with previously published SLC12 structures. A) Schematic representation of the NKCC1 structure (LeuT fold). Scaffold helices are presented in wheat, bundle helices in cyan and the remaining helices presented in grey. B) Comparison of protomer A of the determined hNKCC1 structure (purple) with other published NKCC1 structures (PDB codes: 6NPH, 6PZT; presented in grey) or C) with published KCC structures (PBD codes: 6KKR, 6M1Y, 6UKN, 7D14; presented in grey); D) Comparison of the determined hNKCC1dimer (cyan) with the KCC2 dimer (PDB code 6M23; grey). E) Density for potential cholesterol binding site 1, 2, 3 and 4 in the published KCC3 structure (PDB entry: 6M22).

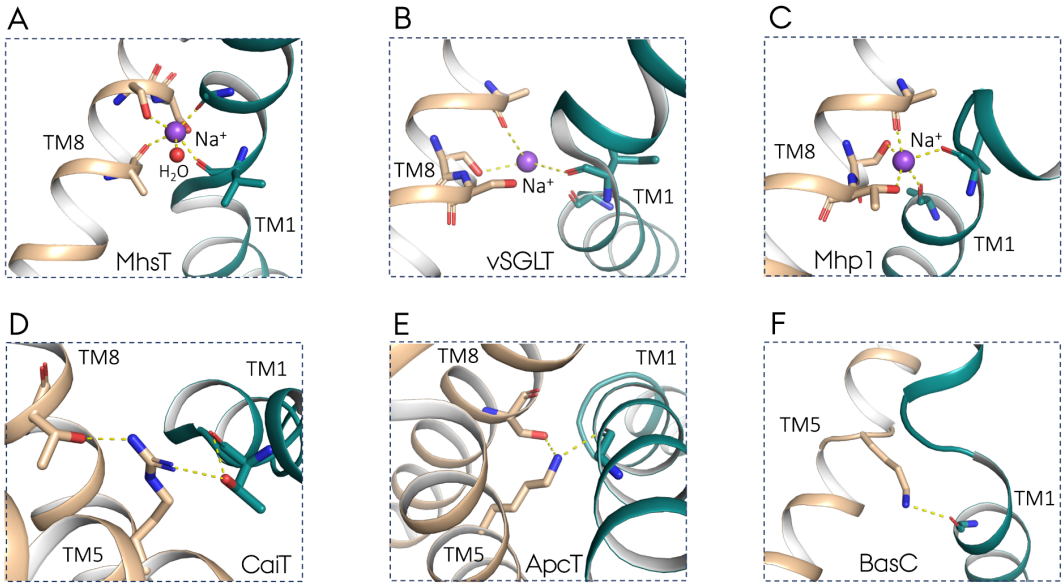

Appendix Figure S3: Na2 binding site in sodium-dependent and sodium (A-C) and sodium-independent (D-E) APC transporters. A) NSS family: MhsT (occluded inward-facing, PDB code: 4US3), B) SSS family: vSGLT (inward-open, PDB code: 3DH4) C) NCS1 family: Mhp1 (occluded ligand bound, PDB code: 4D1A), D) BCCT family: CaiT (inward-facing, PDB code: 2WSW), E) APC family: ApcT (inward-open, PDB code: 3GI9), F) LAT family: BasC (inward-open, PDB code: 6F2W).

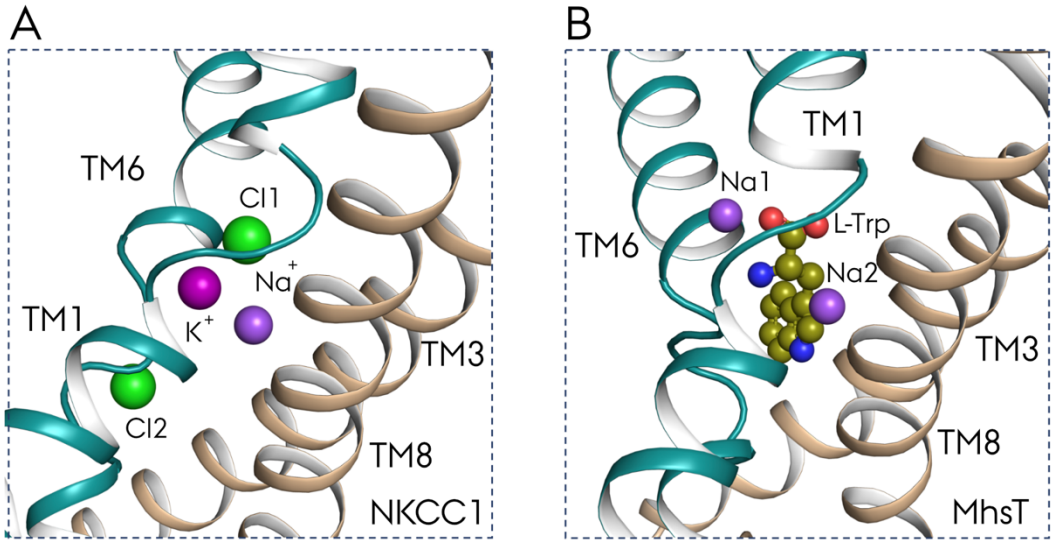

Appendix Figure S4: Substrate binding of SLC12 and SLC6 transporters. Similar substrate binding in the interface between the scaffold (wheat) and bundle domain (cyan) of A) NKCC1 belonging to the SLC12 family and B) MhsT belonging to the SLC6 family (PDB code: 4US3). The potassium ion is presented as a magenta sphere, the sodium ions are presented as purple spheres, the chloride ions are presented as green spheres and the tryptophan substrate of MhsT is presented as brown spheres.

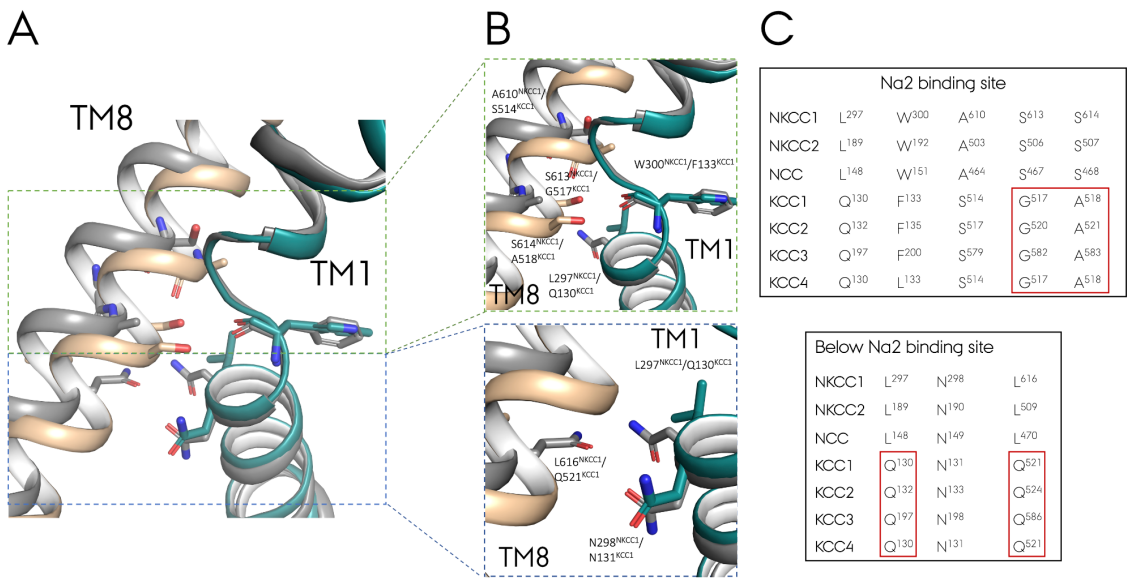

Appendix Figure S5: Lack of a sodium binding site in KCC transporters. A) Superposition of TM1 and TM8 in NKCC1 and KCC1, B) Comparison of Na2 binding site and the part below the Na2 binding site of NKCC1 and KCC1, C) Sequence alignment of the Na2 binding site and the fragment below the Na2 binding site of the CCC transporters. The G-A substitution of KCC1-4 on TM8 responsible for abolishment of sodium binding is highlighted as well as the two Q residues on TM1 and TM8 that are a part of the hydrogen binding network holding TM1-TM8 together.

Data collection and processing	Dataset 1	Dataset 2	Dataset 3	Combined map
Magnification	165000 x	165000 x	130000 x	
Voltage (kV)	300	300	300	
Microscope	Titan Krios2	Titan Krios2	Titan Krios	
Electron exposure (e-/Å^2)	40.12	39.78	60.438	
Defocus range (μm)	0.6-1.6	0.6-1.6	0.5-2.4	
Pixel size	0.507	0.507	0.829	
Camera	Gatan K3 Summit camera	Gatan K3 Summit camera	Gatan K3 Summit camera	
Number of movies	10335	9464	6490	
Symmetry imposed	C2	C2	C2	C2
Initial particle images (no.)	1002976	1566691	2710603	
Final particle images (no.)	81946	56870	119975	256791
Map resolution (Å)	2.79	2.93	2.96	2.55
FSC threshold	0.143	0.143	0.143	0.143
Map resolution range (Å)				2.4-3.6

Model refinement PDB: 7ZGO	
Model composition	
Protein residues	940
Ligands	8
B factors (Å^2)	
Protein	61.44
Ligand	68.87
R.m.s. deviations	
Bond lengths (Å)	0.003
Bond angles (°)	0.531
Ramachandran plot	
Favored (%)	96.58
Allowed (%)	3.42
Disallowed (%)	0
EMRinger Score	3.59

Appendix Table S1: Cryo-EM data collection, refinement and validation.